Exciplex Enhancement as a Tool to Increase OLED Device Efficiency.

Przemyslaw Data,[†,‡] Aleksandra Kurowska,[‡] Sandra Pluczyk,[‡] Pawel Zassowski,[‡] Piotr Pander,[†] Rafal Jedrysiak,[‡] Michal Czwartosz,[‡] Lukasz Otulakowski,[§] Jerzy Suwinski,[§] Mieczyslaw Lapkowski,[‡] Andrew P. Monkman[†]*

[†] Physics Department, University of Durham, South Road, Durham DH1 3LE, United Kingdom.

[‡] Faculty of Chemistry, Silesian University of Technology, M. Strzody 9, 44-100 Gliwice, Poland

ABSTRACT

Organic electronics, mainly due to advancements in OLED (Organic Light Emitting Diode) technology, is a fast developing research area having already revolutionized the displays market. This direction presents the use of exciplex emitters and thermally activated delayed fluorescence (TADF) in OLEDs, to give efficient, stable emitters that do not use scarce and expensive materials such as iridium. Here, it is shown for the first time several diketopyrrolopyrrole (DPP) derivatives that could be used as emitters in OLED devices. We were able to improve the of efficiency DPP materials by forming exciplex enhanced OLED devices. These organic materials were also characterized by electrochemical and spectroscopic methods in order to elucidate each molecule's interaction and decreasing the photoluminescence efficiency.

1. Introduction

DPP derivatives have attracted considerable research interest over the last few years due their significant synthetic and spectroscopic advantages. Specifically, these type of compounds can act as strong acceptor units, exhibit high fluorescence quantum yields, and possess exceptional thermal and photostability, making them excellent building blocks for many applications such as organic electronics,[1-3] solid state lasers,[4,5] dye-sensitized solar cells,[6,7] dyes[8-10] and fluorescent probes.[11] The DPP unit has a well-conjugated structure with a strong π–π interaction and electron-withdrawing effect, which results in efficient charge transport. Relatively low-lying HOMO and LUMO levels also make the DPP unit a promising candidate for application in bulk heterojunction (BHJ) solar cells,[12-19] with further application stemming from their ability to be used as both small molecules[20-23] or copolymers.[24-27] In many publications, the DPP derivatives have been highlighted as a good emitter for OLED devices but nevertheless small molecule OLEDs based on such compounds have not been investigated, despite their very high intensity and PLQY in solution. Unfortunately, DPP derivatives demonstrate strong π-stacked aggregation that may lead to dissipative intermolecular charge transfer and aggravate charge recombination that quenches fluorescence. One of the recent way to improve OLED efficiency it to employ the E-type delayed fluorescence (Thermally Activated Delayed Fluorescence - TADF). A neglected process in OLEDs, has been shown to work very efficiently in converting triplets into singlets in organic exciplex molecules.[28-30] One of the representatives of the TADF emitters are exciplexes. Exciplexes provide simple possibilities to make a wide range of emitters because the wavelength of the emission in such systems is not dependent on the band-gap value of a single compound, but the HOMO-LUMO offset between donor and acceptor molecules. A small range of exciplex TADF materials and devices has been

reported, yielding very high external quantum yields, reaching a leading value of 19% EQE, clearly indicating that very efficient triplet harvesting is occurring and that 100% internal quantum efficiency is possible.[31,32]

In our work, we present the first DPP derivative (**Scheme 1**) based OLED devices and explain how it's possible to increase the overall efficiency employing exciplex moiety.[33-35]

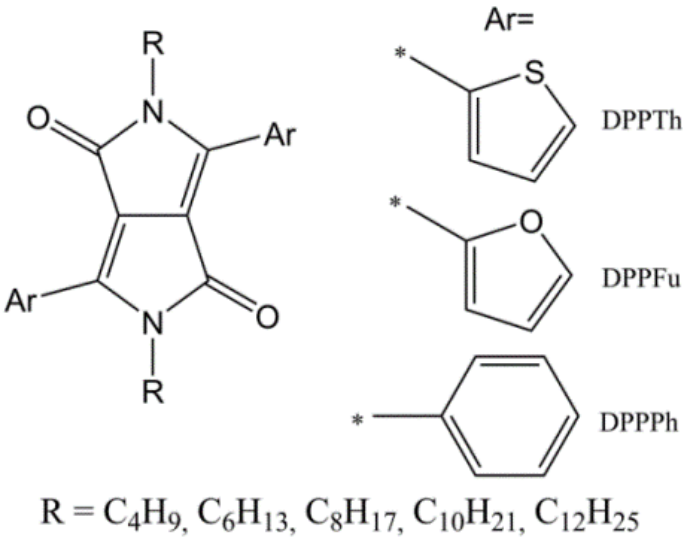

Scheme 1. Compounds studied in this work.

2. Results and Discussions

All of the synthesised DPP compounds were initially investigated using cyclic voltammetry to calculate the ionization potential (IP) and electron affinity (EA) (**Figure 1a,b, Table S1**).[36-38] Reduction proceeds as a two-step process. The first step occurs at a potential lying in the range from -1.88 V to -1.72 V and is reversible in each case, while the second step is irreversible for all of investigated molecules and occurs from -2.52 V to -2.36 V. The reduction process is slightly shifted to higher potentials with increasing number of carbons in the alkyl chain for derivatives from 4 to 10 carbon atoms, while further chain extension lowers the

reduction potential. Furthermore the reduction potential increases in the order: DPPPh< DPPFu< DPPTh (comparing the derivatives with the same alkyl chain), highlighting the donor moieties influence on the reduction process. The impact of the alkyl chain and donor moieties on the oxidation process is similar to the reduction. The oxidation process occurs at higher potential for derivatives with longer alkyl chains, with highest potential observed for derivatives with 10 carbon atoms, while introduction of more carbon atoms in alkyl chain resulted in lowering of the potential of oxidation. The effect of donor moieties on the oxidation potential also follows the reduction, with the lowest potential of oxidation observed for thiophene derivatives. Thiophene and furan derivatives show similar values of band gap energies, whereas phenyl derivatives possess higher band gaps. These data are presented in Table S1.

To explain the effect of structure on their electronic properties, DFT calculations were performed on model compounds containing alkyl chains of 2 carbons long (**Scheme S4**). In case of DPPPhC2, a large dihedral angle of 41.86^{o} was observed between the DPP core and phenyl ring. Since such a large angle has not previously been reported for similar non *N*-alkylated molecules[39,40] one can conclude that interactions between hydrogen atoms on the phenyl rings and *N*-alkyl chains are responsible for non-planar geometry found in DPPPhC2 (**Table S2, Figure S1**).[41] For both DPPFuC2 and DPPThC2, dihedral angles between the DPP core and substituents were found to be only 1.53^{o} and 1.80^{o}, respectively. As a result it can be concluded that 5-membered rings do not create as much steric hindrance as phenyl rings, leading to close to planar geometry. The shape and position of frontier orbitals are presented as an inset in Figure 2b. DPPThC2 and DPPFuC2 have a very similar value of HOMO of -5.43 and -5.39 eV respectively while the HOMO of DPPPhC2 is lower and equal to -5.71 eV. A similar situation can be seen in the case of the LUMO energy level, where DPPThC2 and DPPFuC2 have a

similar value of -2.97 and -2.91 eV respectively while DPPPhC2 departs with the LUMO equating to -2.82 eV (Figure 1). These data indicate that the degree of conjugation is similar in the case of DPPThC2 and DPPFuC2, while molecule DPPPhC2 is conjugated to a lesser extent. These observations coincide well with experimental data

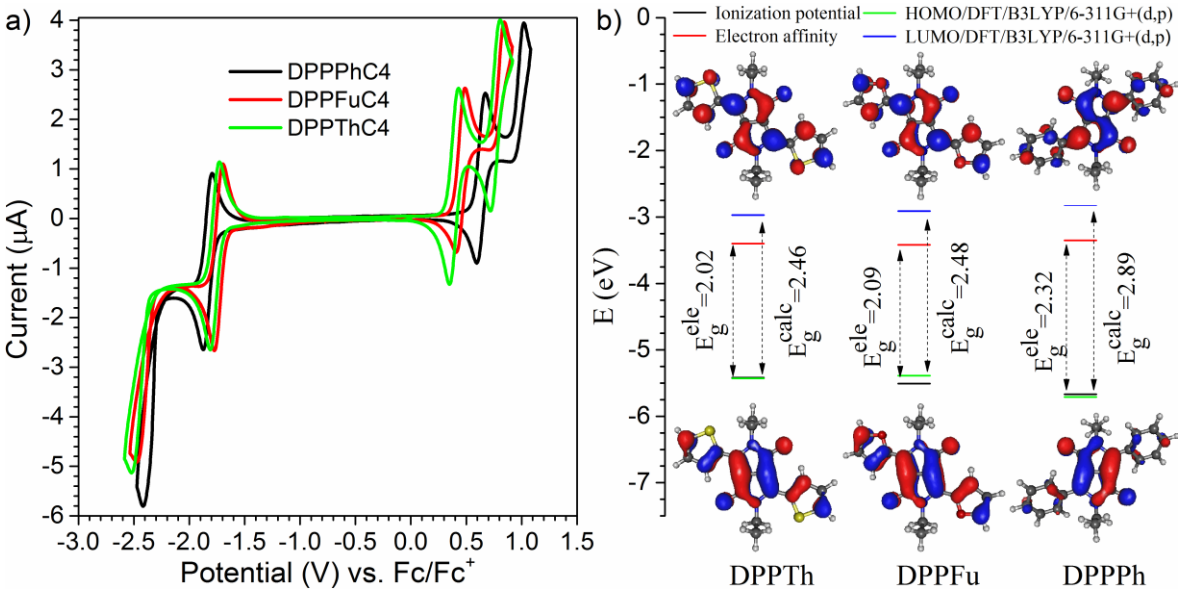

Figure 1. Cyclic voltammograms for both oxidation and reduction reactions of investigated compounds with C4 alkyl chain, representative for all investigated molecules and b) comparison of data from electrochemical experiments with values obtained from DFT calculations. The inset shows the shape of HOMO (lower) and LUMO (upper) orbitals for model compounds with C2 alkyl chains. The value of isocontour is equal to 0.03 in each case.

The UV-vis absorption and fluorescence spectra of DPP derivatives are shown in **Figure 2a,b** and their representative spectral parameters are collected in **Table S3**. The shape and position of optical spectra were not influenced by the length of the *N*-alkyl chain. DPPTh and DPPFu series show two vibronic maxima in their absorption spectra in dichloromethane solution. In both cases, the main absorption band in the range of 450 – 575 nm is split into two well-

defined peaks. The peaks at 549 nm for DPPTh and 538 nm for DPPFu are assigned to the 0-0 vibronic transition and is more intense than the 0-1 transition found at higher energies (Figure 2).[42,43] The exacts positions of separated peaks probably originating from the well-ordered structure of DPPFu and DPPTh. For DPPPh series, the vibronic structure is not well defined which is probably assigned to the weaker rigidity of the conjugated system.[44,45] It is worth noticing that the vibration modes are also present in non-substituted alkyl side chains DPPPh derivatives.[46] Comparing UV-vis spectra of DPP derivatives reveals that the absorption maxima strongly depends the donor unit in monomer backbone. In case of UV-vis spectrum, DPPTh and DPPFu derivatives show similar properties, with first observed transition maximum at 548 and 538 nm, respectively. Replacement of 5-membered rings with phenyl rings results in a hypsochromic shift of the absorption band to a peak maximum of 466 nm caused by the stronger electron donating character of thienyl and furanyl units compared to phenyl substituent, as well already discussed in terms of the twisted molecular structure of DPPPh derivatives. Furthermore, TDDFT calculations were conducted to gain information about these described optical transitions. These data are given in Table S2. In case of all investigated compounds, the first transition is dominated by, the HOMO-LUMO transition with no contribution from other orbitals.

All examined DPP derivatives are also luminescent, reaching high quantum yield in the range of 0.69-0.79 (Table S3). Analysing obtained data it is observable that the length of the alkyl side chain has an influence on quantum yield. For DPPFu derivatives, the quantum yield increases from 0.79 to 0.81 with increasing length of alkyl side chain (**Table S4**). The same phenomenon is observable in the case of DPPPh derivatives. Quantum yield values are also strongly related to an atom's electronegativity within the donor unit and the heavy atom effect.[47]

Comparing DPPFu and DPPTh, the sulfur present in the donor moiety is less electronegative than oxygen, resulting in lower quantum yields (Table S3). The fluorescence spectra of DPP derivatives are usually characterized by a small Stokes shift[48] which is assigned to their planar structure.[49] For DPPTh and DPPFu, the Stokes shift is situated in a range of 11 and 7 nm, respectively (Table S2). In the case of DPPFu, the smaller Stokes shift is caused by, a better interaction between the oxygen in the donor units and hydrogens in alkyl side chains. The strong attraction between these two atoms (O···H) leads to slightly a more planar conformation, as already confirmed by ground state DFT calculations. Hence, the change in conformation between the ground state and the excited state is rather small. In the case of DPPTh, the sulphur atoms in the thiophene units are positively charged and are repelled by the positively charged hydrogen on the side chains,[50] leading to a more pronounced change in conformation in its excited state. In the case of DPPPh the Stokes shift in range of 63 nm indicates that the geometry of the excited state is changed in a significant way compared to the ground state[51] and probably involves the planarization of molecules, reducing the substantial dihedral angle between the DPP core and phenyl substituents.

Spectroelectrochemical measurements were performed to examine the influence of applied potential on the spectroscopic properties of investigated DPP derivatives. This analysis is important for OLED materials which perform under an electrical field.

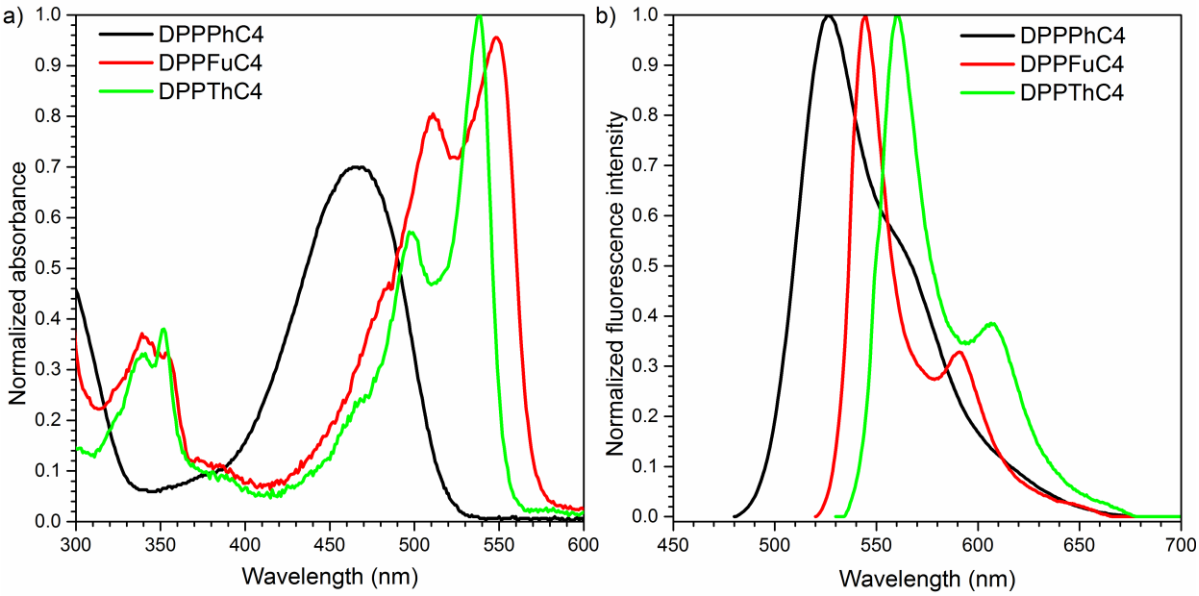

Figure 2. UV-vis (a) and photoluminescence (b) spectra of selected compounds investigated in this study; a representative for all molecules.

All examined compounds underwent reversible oxidation and reduction process, creating stable charged species such as radical cations or anions. The stability of those forms allowed for their spectral characterization and comparison. Some important differences between positive and negative charged speciescan be seen upon investigation of the DFT simulated geometries. Using DPPPhC2 as an example when the charge is set to +1 (radical cation), the dihedral angle is slightly reduced to a value of 39.09°, whereas setting the charge to +2 (dication) results in further reduction of the dihedral angle value to 29.87°. Planarization also occurs when the charge of DPPPhC2 is set to -1 (radical anion). However, the extent of this phenomenon is greater than in the cationic species as the dihedral angle in this example is reduced significantly, to a value of 20.39°. Those differences are however not seen in DPPThC2 and DPPFuC2 since these compounds are planar already in their ground state (**Table S5**).

Spectroelectrochemical measurements were performed to examine the influence of applied potential on the spectroscopic properties of investigated DPP derivatives. This analysis is important for OLED materials which performunder an electrical field. The evolution of the optical spectra during electrochemical oxidation of examined compounds was recorded as a function of applied potential in accordance with cyclic voltammetry (Figure 1a). As the potential is sequentially increased the intensity of the π-π* transition diminishes (**Figure 3**), along with the formation of new peaks at lower energy regions of the spectrum at 670 nm for DPPPhC4, at 605 nm, 860 nm and 1075 nm for DPPFuC4 and at 602 nm, 755 nm, 792 nm and 855 nm for DPPThC4. This effect is assigned to the oxidation process, in which new charge carriers are created. When a potential was applied on the second peak, it resulted in further changes in the optical spectra. In case of DPPThC4, newly formed bands drop while absorbance rises at awavelength of 400 nm. Similar behaviour can be seen in the case of DPPFuC4, however with the formation of a new band at 730 nm. DPPPhC4 tends to lose intensity in the whole range of wavelength. Described changes in the spectra are connected with the formation of a dication in the case of DPPThC4, as absorption band this species is located in the area of 400nm. This is not true for DPPFuC4 and DPPPhC4 since these compounds do not possess a reversible second oxidation peak, as shown by cyclic voltammetry. Those changes are probably connected with the formation of products of irreversible oxidation.

Upon reduction of DPP derivatives, the intensity of the absorption signal corresponding to the neutral molecules gradually decreases whereas new absorption bands are created. The absorption band centered around 600-633 nm is characteristic for the radical anion of *N*-substituted DPP derivatives. In all cases, the absorption spectra of reduced DPPs consist of three

well-defined bands at 600-633 nm, 745-829 nm and 811-935 nm (Figure 3a-f). These similar changes in spectra are caused by the same reduction mechanism that takes place in DPP core.

TDDFT calculations on the geometry of charged species were conducted to explain the origin of newly created optical transitions. These results are presented in Figure 3a-f as vertical bars indicating the wavelength of the calculated transition. For radical cations, TDDFT predicted two new transitions with substantial oscillator strength; HOMO to SOMO at shorter wavelength and SOMO to LUMO at a longer wavelength. In case of DPPPhC2, those excited states also possess a certain amount of HOMO-5 to SOMO transition. In the case of DPPThC2, optical transitions for a molecule charged to +2 were also calculated since compounds with this core showed a reversible second oxidation peak. The most important excited states are located at 385 and 294 nm, with major transitions from HOMO-5 to HOMO and HOMO-2 to LUMO+1, respectively. Calculations of optical spectra of radical anions of investigated compounds result in two excited states, similarly to the case of radical cations.

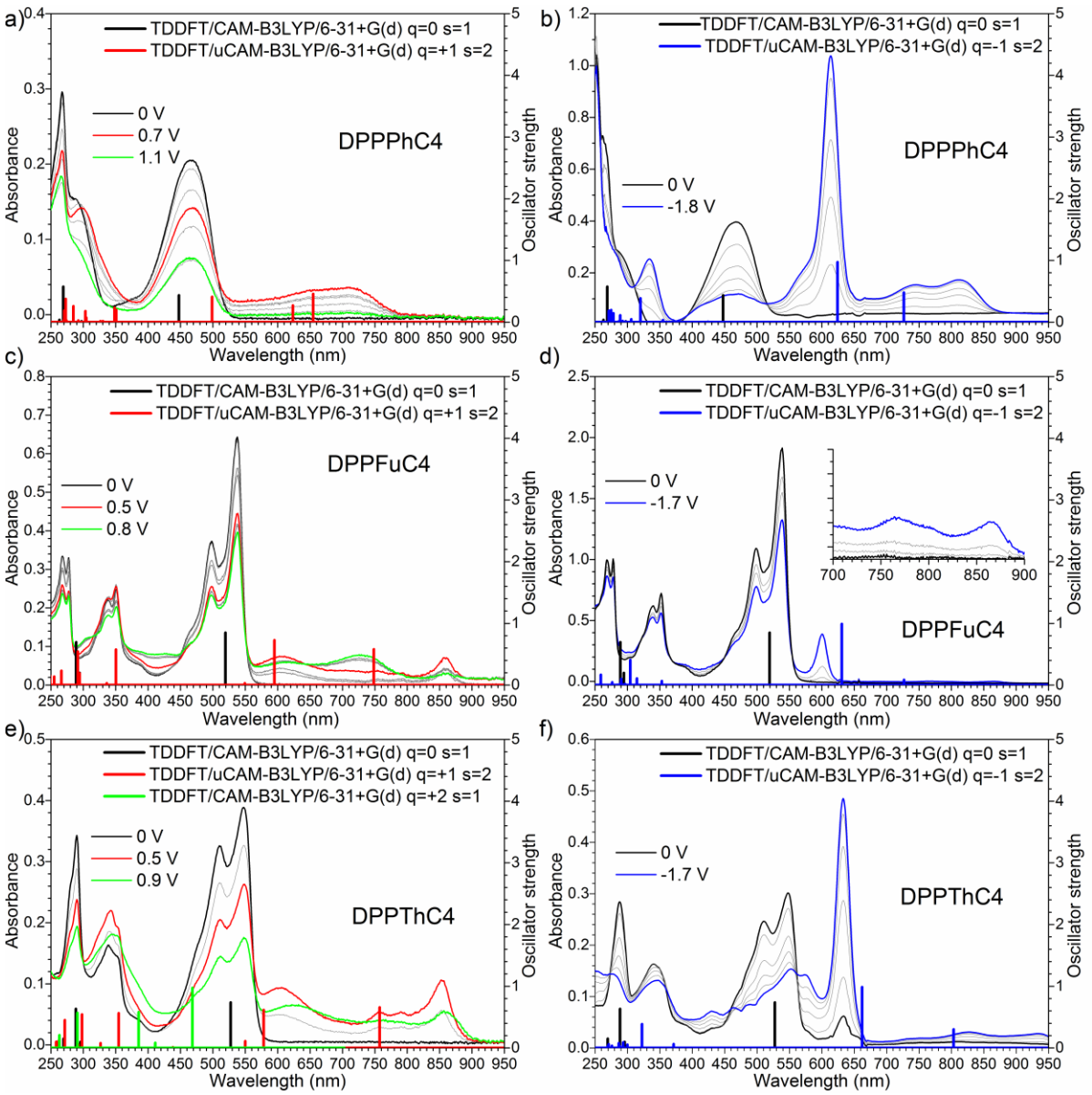

Figure 3. UV-vis-NIR spectra recorded during electrochemical oxidation (left side) and reduction (right side), for compounds: a) and b) DPPThC4, c) and d) DPPFuC4, e) and f) DPPPhC4, together with TDDFT simulated optical transitions.

Comparison of calculated optical transitions with spectroelectrochemical results can produce interesting conclusions. While TDDFT predicted two new bands at a charge of +1 in each case,

one can observe three in experimental spectra. The third band is connected with the occurrence of an additional form of investigated compounds, not included in calculations. These may include for example σ-dimers or π-dimers.

Further analysis of charged species was possible through the use of EPR spectroelectrochemistry. Similarly to other spectroscopic properties, hyperfine coupling constants were not dependent on the length of the alkyl chain. As in other techniques used to characterize charged species, in EPR spectroelectrochemistry one can clearly differentiate between the positive and negative speciesat once. Radical anion EPR spectra of investigated compounds present rich hyperfine structure, originating from interactions of spin with nitrogen atoms on the DPP core and with hydrogen atoms of substituents (details of this are given in **Figure 4**). This indicates that in radical anion molecules spin density is distributed over the entire molecule, which was also confirmed by the DFT simulated spin density (see inset in Figure 4a-f). In the case of radical cations, the analysis is not that simple since these spectra do not present well-separated peaks as an effect of hyperfine interactions, as seen in the radical anion spectra. However based on DFT calculated spin density we proposed a model describing the shape of radical cation spectra, as presented in Figure 4a-f. As it can be seen, one of the reasons for this situation lies in the poor spin density of nitrogen atoms. However, this does not mean that the whole DPP core is free of spin density, which is present on both oxygen and carbon atoms. This indicates that for both radical anion and radical cation, the spin density is distributed entirely over the molecule.

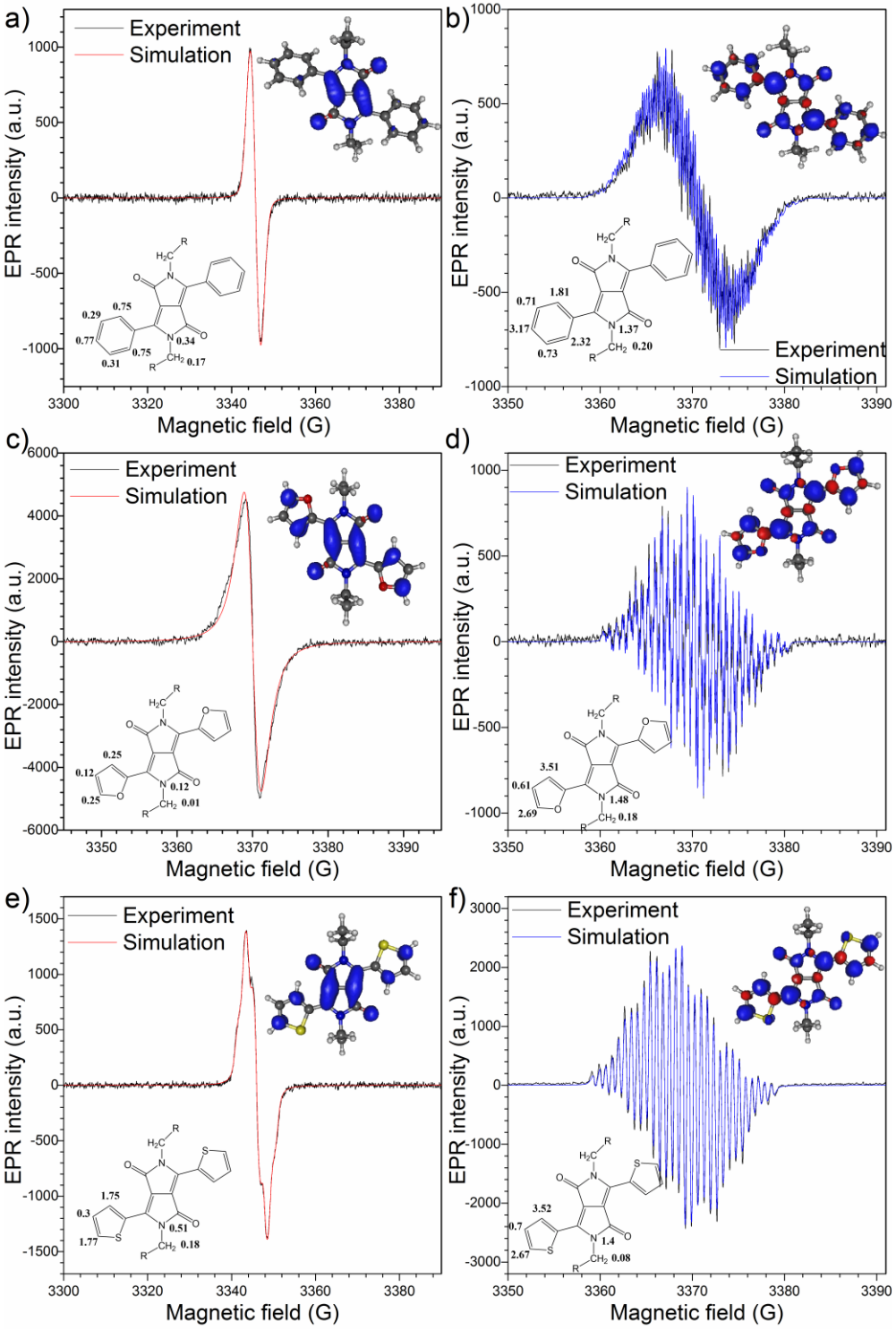

Figure 4. EPR spectra of electrochemically generated radical cations (left side) and radical anions (right side) of investigated compounds: a) and b) DPPThC4, c) and d) DPPFuC4, e) and f) DPPPhC4 together with simulated

spectra. The inset shows hyperfine values used for simulation and DFT calculated spin density for model compounds.

The electrochemical and spectroelectrochemical analysis showed that there is a small influence of alkyl chain upon electronic parameters. EPR spectroelectrochemistry indicates that for both radical anion and radical cation, the spin density is distributed entirely over the molecule resulting strong interaction between molecules which increase the possibility of π-π stacking and σ-dimer formation. Both of these intermolecular formations could negatively influence OLED device performance based on DPP emitters. The several OLED structures were investigated (**Figure 5**) but resulted in similar EQE efficiency lower than 0.4% (the EQE for pure DPP emitters).

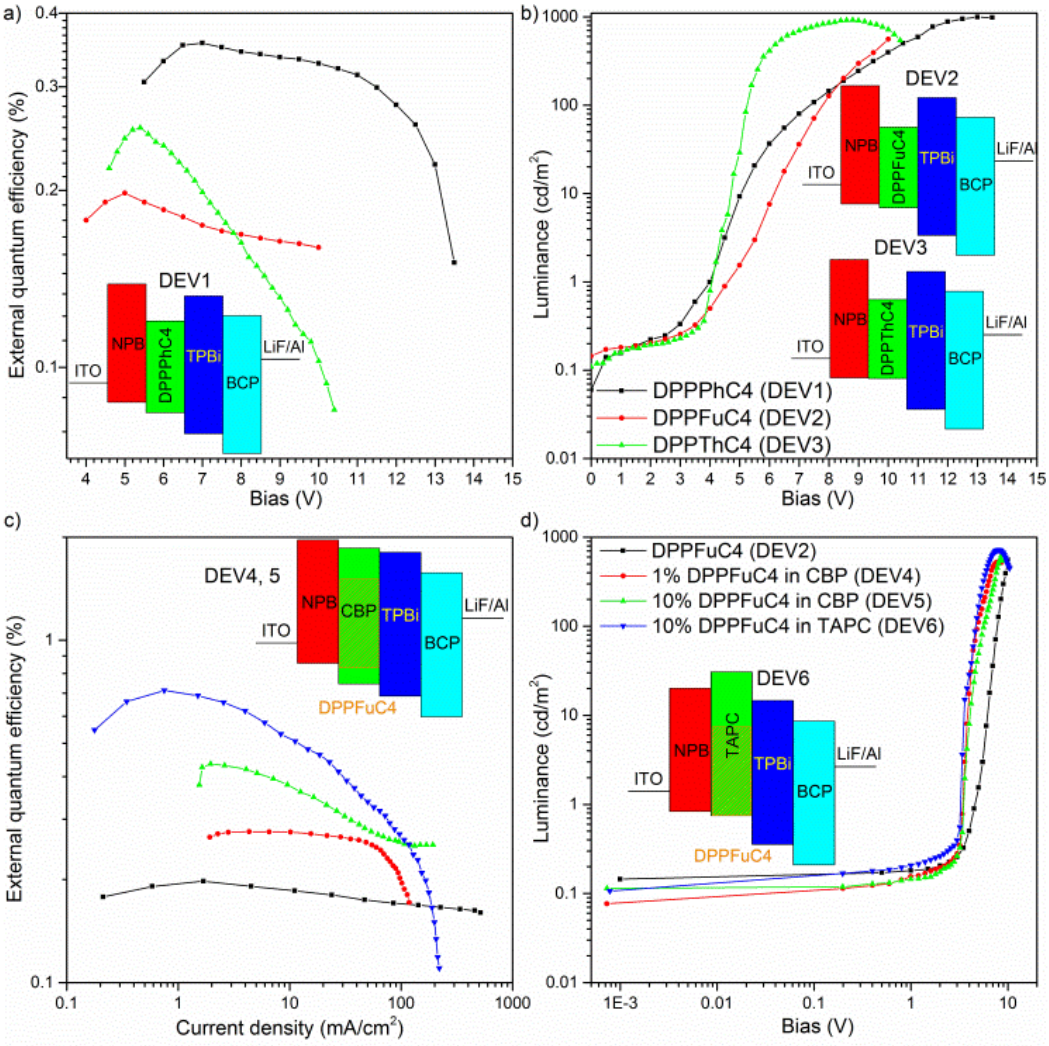

Figure 5. DPP based OLED characteristics. a) EQE vs bias, b) luminance vs bias, insets are OLED structures. DPPFuC4 in TAPC and in CBP OLED characteristics. c) EQE vs current density, d) luminance vs bias, insets are OLED structures.

From an investigative point of view ITO/NPB (40 nm)/DPPPhC4, DPPFuC4 or DPPThC4 (30 nm)/TPBi (20 nm)/BCP (20 nm)/LiF (1 nm)/Al (100 nm) structures were chosen for comparison (Figure 5a,b).The characteristics of donor-host OLED structures (Figure 5c,d - DEV4-6, ITO/NPB (40 nm)/ x% DPPFuC4 in TAPC or CBP (30 nm)/TPBi (20 nm)/BCP (20 nm)/LiF (1

nm)/Al (100 nm)) revealed a high influence of host upon device performance. Although, the luminance was similar for all of the devices, the efficiency improves 2 times in a CBP matrix (10% of DPPFuC4) and 3.5 times in a TAPC matrix. As TAPC is an Electron Blocking Layer (EBL), it wasn't possible to investigate lower %compositions of DPPFuC4 inside this matrix. As a final step, the attempt of deposition of exciplex enhanced TADF device was undertaken. The previously investigated 2d:TAPC exciplex device were chosen due to its high efficiency (>15%).[33] The electroluminescence spectra of the 2d:TAPC device lay at the same wavelength as absorption bands of investigated DPP derivatives (**Figure 6a**) which should allow to direct excitation of DPP compounds by the exciplex. The time-resolved photoluminescence analysis of exciplex enhanced layers proved the occurrence of the delayed component (**Figure S2**).

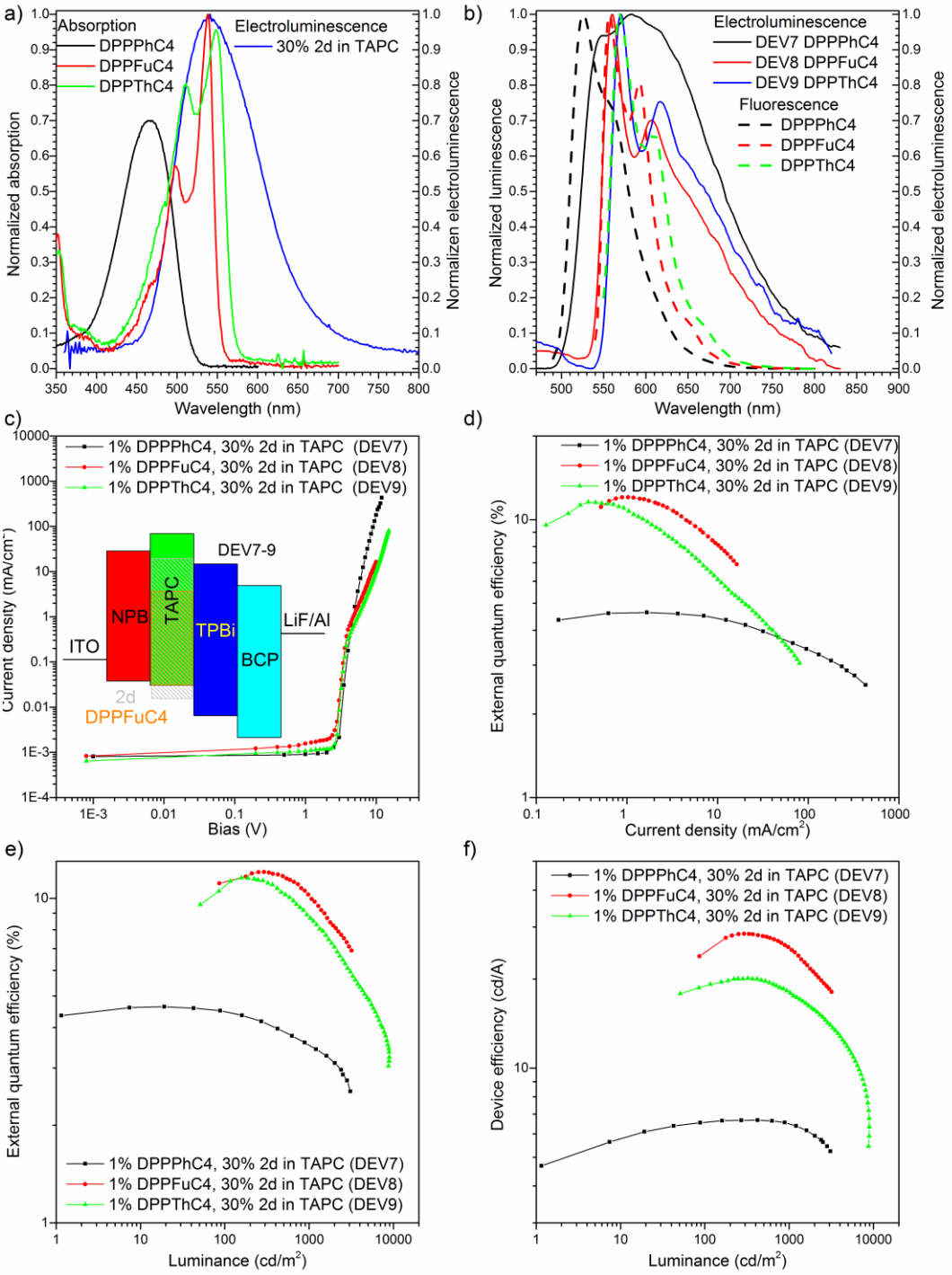

Figure 6. The comparison of the 2d:TAPC OLED device electroluminescence with absorption spectra of DPP molecules (a), comparison of fluorescence of DPP molecules and electroluminescence spectra of exciplex enhanced DPP based OLED devices (b). The characteristic of OLED based on 1% DPPThC4 or DPPFuC4 or DPPPhC4 ,

30%2d in TAPC OLED characteristics. Current density vs bias (c), inset is an OLED structure. EQE vs current density (d), EQE vs luminance (e), device efficiency vs luminance (f).

By using the triple-evaporation technique, several devices were formed (DEV7-9, ITO/NPB (40 nm)/ 1% DPPPhC4, DPPFuC4 or DPPThC4, 30% 2d in TAPC (30 nm)/TPBi (20 nm)/BCP (20 nm)/LiF (1 nm)/Al (100 nm)). The electroluminescence of formed devices were similar to the fluorescence of the pure compound (Figure 6b), only the emission of DPPPhC4 devices were shifted. Due to the fact that absorption maxima of DPPPhC4 is shifted to higher energies (460 nm) than exciplex emission (550 nm) the DPPPhC4 couldn't be fully excited and the electroluminescence of DEV7 contained mixed emission of DPPPhC4 and some exciplex emission (Figure 6b – black line).

In all of the cases, the overall efficiency of exciplex enhanced devices were much higher (Figure 6c-f). It was possible to receive 11.2% for DPPFuC4 and 11.1% for DPPThC4 EQE at 100 cd/m^2 . The best overall efficiency was observed for DPPFuC4 based devices with a 12.1% EQE and 28.4 cd/A device efficiency.

The highest luminance was observed for the thiophene derivative DPPThC4 at 9983 cd/m^2. The efficiency of DPPPhC4 was much smaller mainly, as previously mentioned, due to mixed emission from the exciplex and the DPPPhC4 material.

3. Conclusion

In summary, we conclude that all investigated compounds are electroactive, and don't form polymeric layers during electrical oxidation. Our analysis showed that there is almost no

influence of alkyl chain upon electronic parameters and that there is strong interaction between molecules which increase the possibility of π-π stacking and σ-dimer formation. Spectroelectrochemical analysis showed the strong influence of electric field on electronic properties of molecules and the formation of charge carriers. Electrochemical and spectroelectrochemical analysis showed the strong stability of the compounds and no by-side reaction when upon electric field application. We were also able to improve quite substantially the overall device efficiency firstly by "diluting" DPP compounds in TAPC and CBP hosts and finally by creating exciplex enhanced OLED devices resulting the EQEs higher than 12% when for pure compound it was 0.2%.

ASSOCIATED CONTENT

Details of materials and synthesis. Details of experimental methods. Spectroscopic characteristic of DPP derivatives. TDDFT calculation results. This information is available free of charge via the Internet at http://pubs.acs.org

AUTHOR INFORMATION

Corresponding Author

* email: Przemyslaw.Data@dur.ac.uk; Phone: +441913343590;

ACKNOWLEDGEMNT

This work was supported by the Polish Ministry of Science and Higher Education project no. IP2012 039572. The research leading to these results has received funding from the H2020-MSCA-IF-2014/659288 project "TADFORCE". This research was supported in part by PL-Grid

Infrastructure. P. Z., S.P. and A. K. are scholars supported by the “Doktoris–scholarship program for an innovative Silesia”, co-financed by the European Union within the European Social Fund.

REFERENCES

(1) Sonar, P.; Ng, G. M.; Lin, T. T.; Dodabalapur, A.; Chen, Z. K. Solution Processable Low Bandgap Diketopyrrolopyrrole (DPP) Based Derivatives: Novel Acceptors for Organic Solar Cells. *J. Mater. Chem.* **2010**, *20,* 3626-3636.

(2) Bijleveld, J. C.; Karsten, B. P.; Mathijssen, S. G. J.; Wienk, M. M.; de Leeuw, D. M.; Janssen, R. A. J. Small Band Gap Copolymers Based on Furan and Diketopyrrolopyrrole for Field-Effect Transistors and Photovoltaic Cells. *J. Mater. Chem.* **2011**, *21,* 1600-1606.

(3) Suraru, S. L.; Zschieschang, U.; Klauk, H.; Würthner, F. Diketopyrrolopyrrole as a p-Channel Organic Semiconductor for High Performance OTFTs. *Chem. Commun.* **2011**, *47,* 1767-1769.

(4) Fukuda, M.; Kodama, K.; Yamamoto, H.; Mito, K. Solid-State Laser With Newly Synthesized Pigment. *Dyes Pigments* **2002**, *53,* 67-72.

(5) Fukuda, M.; Kodama, K.; Yamamoto, H.; Mito, K. Evaluation of New Organic Pigments as Laser-Active Media for a Solid-State Dye Laser. *Dyes Pigments* **2004**, *63,* 115-125.

(6) Yum, J. H.; Holcombe, T. W.; Kim, Y.; Rakstys, K.; Moehl, T.; Teuscher, J.; Delcamp, J. H.; Nazeeruddin, M. K.; Grätzel, M. Blue-Coloured Highly Efficient Dye-Sensitized Solar Cells by Implementing the Diketopyrrolopyrrole Chromophore. *Sci. Rep.* **2013**, *3,* 2446.

(7) Li, S. S.; Jiang, K. J.; Zhang, F.; Huang, J. H.; Li, S. G.; Chen, M. G.; Yang, L. M.; Song, Y. L. New Diketopyrrolopyrrole-Based Organic Dyes for Highly Efficient Dye-Sensitized Solar Cells. *Org. Electron.* **2014**, *15,* 1579–1585.

(8) Hao, Z.; Iqbal, A. Some Aspects of Organic Pigments. *Chem. Soc. Rev.* **1997**, *26,* 203-213.

(9) Wallquist, O.; Lenz, R.in *High Performance Pigments*, (Ed.: Faulkner, E.B. Schwartz R.J.) Wiley-VCH, Verlag, 2009, pp. 165–194.

(10) Beninatto, R.; Borsato, G.; de Lucchi, O.; Fabris, F.; Lucchini, V.; Zendri, E. New 3,6-Bis(Biphenyl)Diketopyrrolopyrrole Dyes and Pigments via Suzuki–Miyaura Coupling. *Dyes Pigments* **2013**, *96,* 679-685.

(11) Kaur, M.; Choi, D. H. Diketopyrrolopyrrole: Brilliant Red Pigment Dye-Based Fluorescent Probes and Their Applications. *Chem. Soc. Rev.* **2015**, *44,* 58—77.

(12) Brabec, C.J.; Sariciftci, N.S.; Hummelen, J.C. Plastic Solar Cells. *Adv. Funct. Mater.* **2001**, *11,* 15–26.

(13) Günes, S.; Neugebauer, H.; Sariciftci, N.S. Conjugated Polymer-Based Organic Solar Cells. *Chem. Rev.* **2007**, *107,* 1324–1338.

(14) Thompson, B. C.; Fréchet, J. M. J. Polymer-Fullerene Composite Solar Cells. *Angew. Chem. Int. Ed.* **2008**, *47,* 58–77.

(15) Helgesen, M.; Sŕndergaard, R.; Krebs, F.C. Advanced Materials and Processes for Polymer Solar Cell Devices. *J. Mater. Chem.* **2010**, *20,* 36–60.

(16) Li, Y. Molecular Design of Photovoltaic Materials for Polymer Solar Cells: Toward Suitable Electronic Energy Levels and Broad Absorption. *Acc. Chem. Res.* **2012**, *45,* 723–733.

(17) Scharber, M. C.; Sariciftci, N. S. Efficiency of Bulk-Heterojunction Organic Solar Cells. *Prog. Polym. Sci.* **2013**, *38,* 1929– 1940.

(18) Liu, F.; Gu, Y.; Shen, X.; Ferdous, S.; Wang, H.-W.; Russell, T. P. Characterization of the Morphology of Solution Processed Bulk Heterojunction Organic Photovoltaics. *Prog. Polym. Sci.* **2013**, *38,* 1990-2052.

(19) Feng, H. F.; Fu, W. F.; Li, L.; Yu, Q. C.; Lu, H.; Wan, J. H.; Shi, M. M.; Chen, H. Z.; Tan, Z.; Li, Y. Triphenylamine Modified Bis-Diketopyrrolopyrrole Molecular Donor Materials With Extended Conjugation for Bulk Heterojunction Solar Cells. *Org. Electron.* **2014**, *15,* 2575–2586.

(20) Kylberg, W.; Sonar, P.; Heier, J.; Tisserant, J. N.; Müller, C.; Nüesch, F.; Chen, Z. K.; Dodabalapur, A.; Yoon, S.; Hany, R. Synthesis, Thin-Film Morphology, and Comparative Study of Bulk and Bilayer Heterojunction Organic Photovoltaic Devices Using Soluble Diketopyrrolopyrrole Molecules. *Energy Environ. Sci.* **2011**, *4,* 3617-3624.

(21) Lafleur-Lambert, S.; Rondeau-Gagne, S.; Soldera, A.; Morin, J.-F. Synthesis and Characterization of a New Ethynyl-Bridged C_{60} Derivative Bearing a Diketopyrrolopyrrole Moiety. *Tetrahedron Lett.* **2011**, *52,* 5008-5011.

(22) Chen, T. L.; Zhang, Y.; Smith, P.; Tamayo, A.; Liu, Y.; Ma, B. Diketopyrrolopyrrole Containing Oligothiophene Fullerene Triads and Their Use in Organic Solar Cells. *ACS Appl. Mater. Interfaces* **2011**, *3,* 2275-2280.

(23) Hong, T. R.; Shin, J.; Um, H. A.; Lee, T. W.; Cho, M. J.; Kim, G. W.; Kwon, J. H.; Choi, D. H. New π-Extended Diketopyrrolopyrrole-Based Conjugated Molecules for Solution-Processed Solar Cells: Influence of Effective Conjugation Length on Power Conversion Efficiency. *Dyes Pigments* **2014**, *108,* 7-14.

(24) Falzon, M. F.; Zoombelt, A. P.; Wienk, M. M.; Janssen, R. A. J. Diketopyrrolopyrrole-Based Acceptor Polymers for Photovoltaic Application. *Phys. Chem. Chem. Phys.* **2011**, *13,* 8931-8939.

(25) Li, J.; Ong, K.-H.; Lim, S.-L.; Ng, G.-M.; Tan, H.-S.; Chen, Z.-K. A Random Copolymer Based on Dithienothiophene and Diketopyrrolopyrrole Units for High Performance Organic Solar Cells. *Chem. Commun.* **2011**, *47,* 9480-9482.

(26) Qu, S.; Tian, H. Diketopyrrolopyrrole (DPP)-Based Materials for Organic Photovoltaics. *Chem. Commun.* **2012**, *48,* 3039-3051.

(27) Liang, H.; Zhang, X.; Peng, R.; Ouyang, X.; Liu, Z.; Chen, S.; Ge, Z. Photovoltaic Performance Enhancement From Diketopyrrolopyrrole-Based Solar Cells Through Structure Manipulation. *Dyes Pigments* **2015**, *112,* 145-153.

(28) Zhang, Q.; Li, J.; Shizu, K.; Huang, S.; Hirata, S.; Miyazaki, H.; Adachi, C. Design of Efficient Thermally Activated Delayed Fluorescence Materials for Pure Blue Organic Light Emitting Diodes. *J. Am. Chem. Soc*. **2012**, *134,* 14706-14709.

(29) Kawasumi, K.; Wu, T.; Zhu, T.; Chae, H.S.; Voorhis, T.V.; Baldo, M.A.; Swager T.M. Thermally Activated Delayed Fluorescence Materials Based on Homoconjugation Effect of Donor–Acceptor Triptycenes. *J. Am. Chem. Soc.* **2015**, *137,* 11908-11911.

(30) Albrecht, K.; Matsuoka, K.; Fujita, K.; Yamamoto, K. Carbazole Dendrimers as Solution-Processable Thermally Activated Delayed-Fluorescence Materials. *Angew. Chem. Int. Edit.* **2015**, *54,* 5677-5682.

(31) Goushi, K.; Yoshida, K.; Sato, K.; Adachi, C. Organic Light-Emitting Diodes Employing Efficient Reverse Intersystem Crossing for Triplet-to-Singlet State Conversion. *Nat. Photonics*, **2012**, *6,* 253-258.

(32) Gouchi, K.; Adachi, C. Efficient Organic Light-Emitting Diodes Through Up-Conversion from Triplet to Singlet Excited States of Exciplexes. *Appl. Phys. Lett.* **2012**, *101,* 023306.

(33) Jankus, V.; Data, P.; Graves, D.; McGuinness, C.; Santos, J.; Bryce, M. R.; Dias, F. B.; Monkman, A. P. Highly Efficient TADF OLEDs: How the Emitter–Host Interaction Controls Both the Excited State Species and Electrical Properties of the Devices to Achieve Near 100% Triplet Harvesting and High Efficiency. *Adv. Funct. Mater.* **2014**, *24,* 6178-6186.

(34) Data, P.; Motyka, R.; Lapkowski, M.; Suwinski, J.; Jursenas, S.; Kreiza, G.; Miasojedovas, A.; Monkman, A. P. Efficient *p*-Phenylene Based OLEDs with Mixed Interfacial Exciplex Emission. *Electrochim. Acta* **2015**, *182,* 524-528.

(35) Jankus, V.; Chiang, C. J.; Dias, F.; Monkman, A. P. Deep Blue Exciplex Organic Light-Emitting Diodes with Enhanced Efficiency; *p*-type or *e*-type Triplet Conversion to Singlet Excitons? *Adv. Mater.* **2013**, *25,* 1455-1459.

(36) Data, P.; Motyka, R.; Lapkowski, M.; Suwinski, J.; Monkman, A. P. Spectroelectrochemical Analysis of Charge Carriers as a Way of Improving Poly(*p*-phenylene)-Based Electrochromic Windows. *J. Phys. Chem. C* **2015**, *119,* 20188-20200.

(37) Data, P.; Lapkowski, M.; Motyka, R.; Suwinski J. Influence of Alkyl Chain on Electrochemical and Spectroscopic properties of Selenophenes. *Electrochim. Acta* **2013**, *87,* 438-449.

(38) Bredas, J. L. Mind the Gap! *Mater. Horiz.* **2014**, *128,* 430-438.

(39) Lunak, S.; Vynuchal, J.; Hrdina, R. Geometry and Absorption of Diketo-Pyrrolo-Pyrrole Isomers and Their Pi-Isoelectronic Furo-Furanone Analogues. *J. Mol. Struct.* **2009**, *919,* 239–245.

(40) Lunak, S.; Vynuchal, J.; Horackova, P.; Frumarova, B.; Zak, Z.; Kucerik, J.; Salyk, O. Structure and Raman Spectra of Pyridyl Substituted Diketo-Pyrrolo-Pyrrole Isomers and Polymorphs. *J. Mol. Struct.* **2010**, *983,* 39–47.

(41) Luňák, S.; Eliáš, Z.; Mikysek, T.; Vyňuchal, J.; Ludvík, J. One Electron Vs. Two Electron Electrochemical and Chemical Oxidation of Electron-Donor Substituted Diketo-Pyrrolo-Pyrroles. *Electrochim. Acta.* **2013**, *106,* 351–359.

(42) Luňák, S.; Vyňuchal, J.; Vala, M.; Havel, L.; Hrdina, R. The Synthesis, Absorption and Fluorescence of Polar Diketo-Pyrrolo-Pyrroles. *Dyes Pigments* **2009**, *82,* 102-108.

(43) Luňák, S.; Vala, M.; Vyňuchal, J.; Ouzzane, I.; Horáková, P.; MožÍšková, P.; Eliáš, Z.; Weiter, M. Absorption and Fluorescence of Soluble Polar Diketo-Pyrrolo-Pyrroles. *Dyes Pigments* **2011**, *91,* 269-278.

(44) Blanchard, P.; Brisset, H.; Illien, B.; Riou, A.; Roncali, J. Bridged Dithienylethylenes as Precursors of Small Bandgap Electrogenerated Conjugated Polymers. *J.* Org. Chem. **1997**, *62,* 2401-2408.

(45) Vala, M.; Vyňuchal, J.; Toman, P.; Weiter, M.; Luňák, S. Novel, Soluble Diphenyl-Diketo-Pyrrolopyrroles: Experimental and Theoretical Study. *Dyes Pigments* **2010**, *84,* 176-182.

(46) Vala, M.; Weiter, M.; Vyňuchal, J.; Toman, P.; Luňák, S. Comparative Studies of Diphenyl-Diketo-Pyrrolopyrrole Derivatives for Electroluminescence Applications. *J. Fluoresc.* **2008**, *18,* 1181-1186.

(47) Becker, H. G. O.; Böttcher, H.; Dietz, F.; El9cov, A.; Rehorek, V. D.; Roewer, G.; Schiller, K.; Studzinskij, O. P.; Timpe, H. J. *Einführung in die Photochemie,* Thieme, Stuttgart, New York, 1983

(48) Edman, P.; Johansson, L. B. A.; Langhals, H. Polarized Light Spectroscopy of Dihydro-pyrroledione in Liquids and Liquid Crystals: Molecular Conformation and Influence by an Anisotropic Environment. *J. Phys. Chem.* **1995**, *99,* 8504-8509.

(49) Potrawa, T.; Langhals, H. Fluoreszenzfarbstoffe mit Großen Stokes-Shifts - Lösliche Dihydropyrrolopyrroldione *Chem. Ber.-Rec.* **1987**, *120,* 1075-1078.

(50) Lévesque, S.; Gendron, D.; Bérubé, N.; Grenier, F.; Leclerck, M.; Côté, M. Thiocarbonyl Substitution in 1,4-Dithioketopyrrolopyrrole and Thienopyrroledithione Derivatives: An Experimental and Theoretical Study. *J. Phys. Chem. C* **2014**, *118,* 3953-3959.

(51) Mitschke, U.; Debaerdemaeker, T.; Bäuerle, P. Structure-Property Relationships in Mixed Oligoheterocycles Based on End-Capped Oligothiophenes. *Eur. J. Org. Chem.* **2000**, *2000,* 425-437.

Table of Contents